Research paper

Two polyhedral frameworks of an $M_{12}L_{24}$ spherical complex revealed by replica-exchange molecular dynamics simulations

Yuhei Tachi[a], Sota Sato[b,d], Makoto Yoneya[c], Makoto Fujita[d], Yuko Okamoto[a,e,f,g,h,*]

[a] Department of Physics, Graduate School of Science, Nagoya University, Nagoya, Aichi 464- 8602, Japan
[b] Department of Chemistry, School of Science, The University of Tokyo and Japan Science and Technology Agency, Exploratory Research for Advanced Technology (ERATO), Isobe Degenerate π-Integration Project, 7-3-1 Hongo, Bunkyo-ku, Tokyo 113-0033, Japan
[c] National Institute of Advanced Industrial Science and Technology, 1-1-1 Umezono, Tsukuba 305-8568, Japan
[d] Department of Applied Chemistry, School of Engineering, The University of Tokyo, 7-3-1 Hongo, Bunkyo-ku, Tokyo 111-8656, Japan
[e] Structural Biology Research Center, Graduate School of Science, Nagoya University, Nagoya, Aichi 464-8602, Japan
[f] Center for Computational Science, Graduate School of Engineering, Nagoya University, Nagoya, Aichi 464-8603, Japan
[g] Information Technology Center, Nagoya University, Nagoya, Aichi 464-8601, Japan
[h] JST-CREST, Nagoya, Aichi 464-8602, Japan

HIGHLIGHTS

- Replica-exchange molecular dynamics predicts the framework of a metal-ligand complex.
- The metal-ligand complex has two polyhedral frameworks with T_d and C_{3v} symmetry.
- The metal-ligand complex with T_d symmetry is enthalpically favored.
- The metal-ligand complex with C_{3v} symmetry has the highest probability of existence.

ARTICLE INFO

ABSTRACT

We performed replica-exchange molecular dynamics (REMD) simulations for self-assembly of an $M_{12}L_{24}$ spherical complex that consists of 12 palladium ions (M) and 24 bent ligands (L). We found two metal-ligand frameworks with polyhedral structure were mainly observed with almost equal probability. One of the two frameworks, which has the lowest potential energy, has the same symmetry, T_d, as the framework determined by the X-ray crystallographic analysis. The other framework, which has a slightly higher probability, has a different symmetry, C_{3v}. The latter framework is less likely to be observed experimentally than the former because of the difficulty in crystallization.

1. Introduction

Coordination complexes have attracted much attention over the past decade (for a review, see, e.g. Ref. [1]). For example, well-defined spherical complexes M_nL_{2n} ($n = 2$ [2,3], 6 [4], 12 [5–7], 24 [8], 30 [9,10], and 48 [10]) self-assembled from n metal ions (M) and $2n$ slightly bent ligands (L) have been reported. The n value of these spherical complexes discontinuously varies by changing the bent angle of the ligands [8]. The hollow of the spherical complex can be used as a molecular cage with various functions, e.g., encapsulation of guest molecules [11,12], synthesis of nanoparticles [13], and artificial biomolecular clusters [14]. Hence, the information of the metal-ligand framework of the spherical complexes is important for the development

of designed functions through these chemical modifications. X-ray crystallographic analysis is often used to determinate three-dimensional molecular structures. However, the crystallization in many cases is difficult and requires a lot of time and effort in measurements using synchrotron radiation facilities and analyses. The prediction of the polyhedral framework of the M_nL_{2n} by using graph theory has been proposed [8,9]. In the polyhedral framework, metal ions correspond to vertices and ligands correspond to sides. Although this method is quite simple, thermodynamic stability of the spherical complex is not considered. Therefore, molecular dynamics (MD) techniques play a role as a prediction tool, which can consider the thermodynamic stability of the spherical complexes. In a previous study, some of the authors developed a coarse-grained model to investigate the self-assembly process
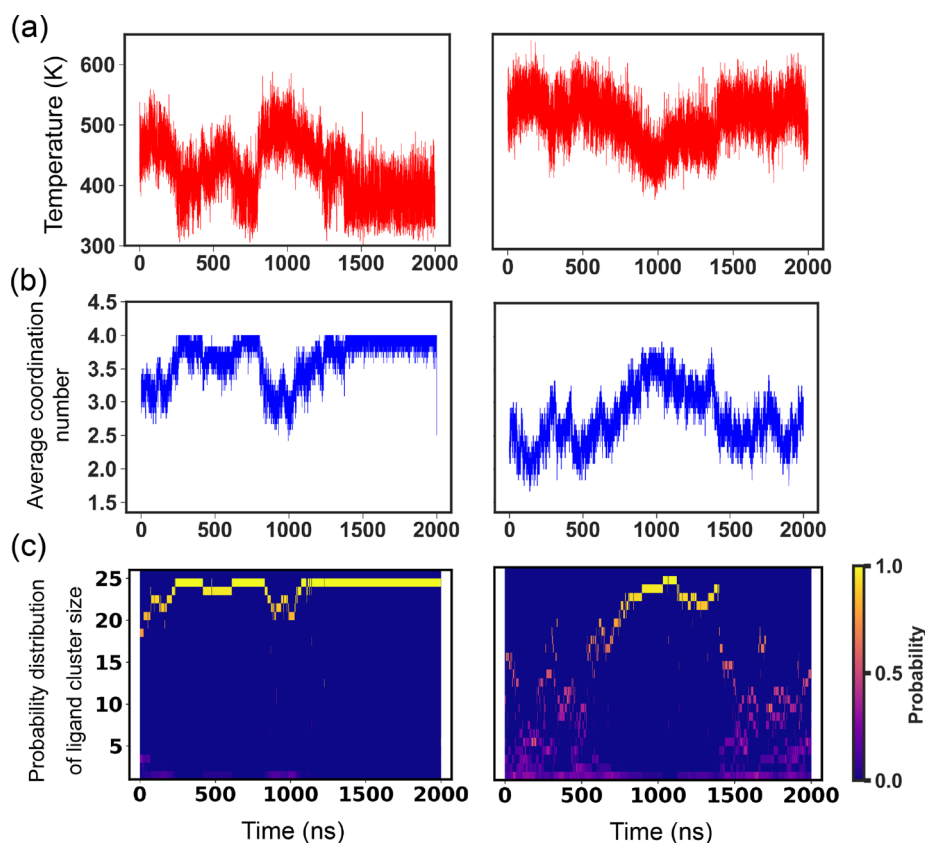
Fig. 1. Time series of physical quantities from two of randomly chosen replicas: (a) temperature, (b) average coordination number, and (c) probability distribution of ligand cluster size.

of the coordination cage M_6L_8 system in dimethyl sulfoxide (DMSO) [15]. Furthermore, MD simulations of the self-assembly process of the coordination cage $M_{12}L_{24}$ system have been reported [16]. That study revealed that the $M_{12}L_{24}$ self-assembly process involves kinetic trapping for smaller-sized clusters, e.g., M_6L_{12}, M_8L_{16}, and M_9L_{18}. In fact, these metastable clusters in the self-assembly process were also reported experimentally [17]. The existence of these metastable clusters motivated us to validate the thermodynamic stability of the $M_{12}L_{24}$ by MD techniques. In recent years, several studies showed the utility of replica-exchange molecular dynamics (REMD) method [18] to predict the self-assembled structures of biomolecules and nanomaterials [19–22]. REMD is one of the most widespread enhanced sampling techniques to investigate rugged free energy landscapes of protein folding. In this study, we performed REMD simulations to validate the thermodynamic stability of the $M_{12}L_{24}$ spherical complex, which has metastable intermediate structures in its self-assembly process.

2. Computational details of REMD simulations

In REMD [18], MD simulations of non-interacting replicas at a range of different temperatures are performed independently and pairs of replicas or, equivalently temperatures, are periodically exchanged. For example, the exchange of i-th replica with temperature T_m and jth replica with temperature T_n gives,

$$X = \{...x_m^{[i]}...x_n^{[j]}...\} \rightarrow X' = \{...x_m^{[j]}...x_n^{[i]}...\}, \quad (1)$$

where $x_m^{[i]}$ is a state of i-th replica with T_m. The exchange probability w is given by the usual Metropolis criterion.

$$w(x_m^{[i]}|x_n^{[j]}) = \min(1, \exp(-\Delta)), \quad \Delta = (\beta_m - \beta_n)\{E(q^{[j]}) - E(q^{[i]})\}, \quad (2)$$

where β is inverse temperature, E is potential energy of each replica, and q is generalized coordinate of each replica. This algorithm allows

each replica to achieve a random walk in the temperature space. This temperature random walk helps the metal-ligand system to escape from metastable intermediate structures.

The initial arrangement of 12 palladium ions and 24 bent ligands was generated randomly. As in the previous studies [15,16], we incorporated 6 explicit solvent atoms of the CH united atom type into the system box randomly. The number of the explicit solvent atoms was the optimum number (half of the palladium ion number) to speed up the formation of the coordination cage M_6L_8 by collision of these solvent atoms [15]. The box size was set to $195.74 \times 195.74 \times 195.74 \, \text{Å}^3$. We used the same coarse-grained model as in the previous MD study [16]. For the metal-ligand coordination interactions, the cationic dummy atom (CaDA) model [23] was used. A coarse-grained solvent model which combines the three methods, Langevin dynamics (LD) [24], generalized reaction field method [25], and Weeks-Chandler-Andersen (WCA) potential [26], was used. MD simulations were performed by the GROMACS (version 4.5.7) program package [27] to which the WCA potential was implemented. We performed REMD simulations with NVT ensemble. The simulation time was $2\,\mu\text{s}$ for each replica and we used 12 replicas, in which 12 temperature values were distributed between 343 K (the experimental temperature) and 543 K: 343.0, 357.6, 372.9, 388.8, 405.4, 422.6, 440.7, 459.5, 479.1, 499.5, 520.8, and 543.0 K. Replica exchange of 12 pairs of temperatures was tried every 10000 MD steps. Equilibration MD runs were performed for 400 ns at each temperature before the REMD simulations. The temperatures were controlled by a stochastic thermostat with the time constant 0.1 ps. LINCS bond constraint [28] with a 4 fs time step was used to keep the stability of the LINCS algorithm at the maximum temperature. The cutoff distance for charge group-based twin-range van der Waals interactions and electrostatic interactions [29] was set to 0.65 nm and 1.4 nm, respectively. All physical quantities were calculated by using the data sampled every 100 ps interval.

3. Results

Fig. 1a shows time series of temperature of two replicas, which were randomly chosen from 12 replicas. This figure shows that each replica achieves a random walk between experimental temperature (340 K) and higher temperatures, which suggests that the REMD simulation performed properly. The results of other replicas were similar. Time series of temperature of all replicas are shown in Fig. S1. Time series of average coordination number per one palladium ion of the two replicas are shown in Fig. 1b. Here, a coordination bond was considered to be formed between palladium ions and ligand-nitrogen atoms if their distance was within 3.6 Å. Fig. 1b shows that a coordination bond tends to be broken at higher temperatures and there is a negative correlation between the temperature and the average coordination number. Time series of probability distribution of ligand cluster size of the two replicas is shown in Fig. 1c. The ligand cluster size was defined as number of ligands contained in a metal-ligand cluster connected by coordination bonds. From this figure, it can be seen that smaller-sized clusters have high probability at higher temperatures. The collapse of clusters at higher temperatures prevents the $M_{12}L_{24}$ system from kinetic trapping at intermediate structures. Time series of the average coordination number and the probability distribution of all replicas are shown in Figs. S2 and S3. A typical replica trajectory of the metal-ligand complex over first 1 μs is shown in Movie S1 of Supplementary material. In fact, we found that the exchange of ligand placements frequently occurs at higher temperatures in this movie. Fig. 2a shows the probability distribution of the ligand cluster size at each temperature.

At the experimental temperature (340 K), we found that the ligand cluster size of 24 has the highest probability in this figure. The average coordination number per palladium ion at each temperature is shown in Fig. 2b. Jackknife method [30] was used for calculating the average values and the standard errors in this figure. This figure shows that the average coordination number is close to 4 at the experimental condition. The ligand cluster size of 24 and the average coordination number of 4 correspond to the features of experimentally observed $M_{12}L_{24}$ [7,8]. A polyhedral framework with T_d symmetry was observed in metal-ligand clusters with ligand cluster size of 24 and average coordination number of 4 (see Fig. 3a). This symmetry is consistent with that of the stereoisomer determined by X-ray crystallographic analysis [7,8]. On the other hand, a polyhedral framework with C_{3v} symmetry was also observed (see Fig. 3b). To discuss more details, differences in the arrangement of the faces surrounding the palladium ions in each framework are shown in Fig. 3c. The faces are constructed from the ligand edges. The framework with C_{3v} symmetry has four palladium ions with distorted ligand placement compared to the framework with T_d symmetry. The framework with C_{3v} symmetry has been reported in the self-assembly of palladium ions and two ligands with different lengths [31]. To assess the convergence of relative probability of two frameworks, we calculated time series of relative probability of metal-
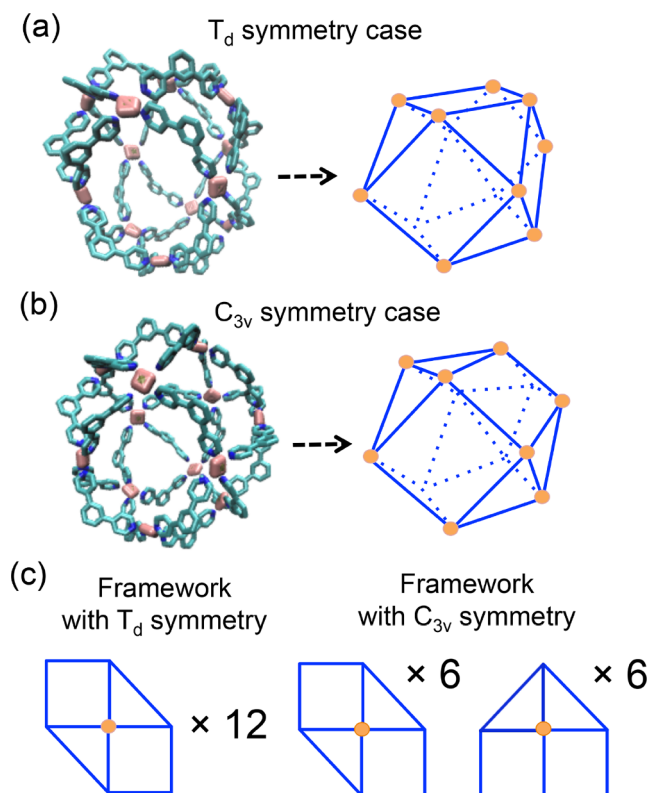

Fig. 3. (a) A polyhedral framework with T_d symmetry. (b) A polyhedral framework with C_{3v} symmetry. (c) Differences in the arrangement of the ligand faces surrounding the palladium ions in each framework (orange points: palladium ions, blue solid lines: ligands).

ligand frameworks with ligand cluster size of 24 and average coordination number of 4 at the experimental temperature (see Fig. S4). The relative probability of each framework was calculated every 10 ns. From this figure, it can be seen that the relative probability values in the first half of the simulation changes drastically. Therefore, the second half of the simulation trajectory was used to calculate the relative probability values and its standard errors by Jackknife method [30]. Relative probability and potential energy of metal-ligand frameworks at the experimental temperature are listed in Table 1. The framework with C_{3v} has the highest probability. The values of the potential energy of framework with T_d symmetry and framework with C_{3v} symmetry were −810(1) kJ/mol and −806(1) kJ/mol, respectively. Hence, the stereoisomer with C_{3v} symmetry is favored entropically but that with T_d symmetry is favored enthalpically. Distorted coordination bonds of the framework with C_{3v} symmetry allow more fluctuations of the ligands than the framework with T_d symmetry. Relative
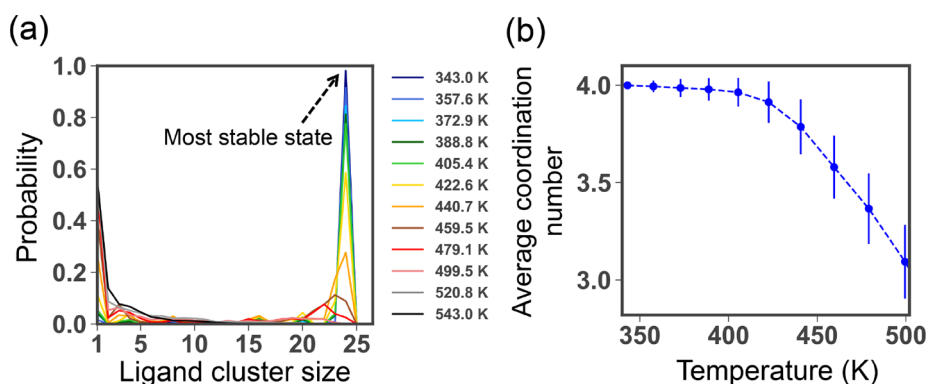

Fig. 2. (a) Probability distribution of ligand cluster size at each temperature. (b) Average coordination number per palladium ion at each temperature.

Table 1
Relative probability and potential energy of metal-ligand frameworks at the experimental temperature (343 K).

	Framework with T_d symmetry	Framework with C_{3v} symmetry	Other frameworks
Relative probability	0.40(3)	0.56(3)	0.04(1)
Potential energy (kJ/mol)	−810(1)	−806(1)	−782(4)

probabilities of the two frameworks have closer average values than other frameworks. We believe that our force field is accurate enough to distinguish the two low-energy frameworks (namely, the one with T_d symmetry and the other with C_{3v} symmetry) from other frameworks with high energy. However, it may be difficult to decide definitely whether which of the two low-energy frameworks have lower free energy. To more accurately estimate the free energy difference between the two stereoisomers, it is necessary to consider quantum effects of the metal-ligand coordination interactions. We remark that the two stereoisomers are very difficult to distinguish from each other by the experimental methods such as the nuclear magnetic resonance (NMR) and the mass spectrometry (MS). Because C_{3v} symmetry has fewer symmetric elements than T_d symmetry, it will be more difficult to crystallize the stereoisomer with C_{3v} symmetry than that with T_d symmetry, which can explain why we observe mostly the stereoisomer with T_d symmetry in the X-ray crystallographic analyses [7,8,12,17,32–34]. Therefore, we conjecture that both stereoisomers exist as (meta) stable states but it is more difficult to detect one experimentally than the other.

Movie S1. A typical first 1-μs trajectory of one of the replicas from the REMD simulation of the metal-ligand complex, $M_{12}L_{24}$.

4. Conclusions

We performed REMD simulations of metal-ligand self-assembly to validate the thermodynamic stability of the spherical complex $M_{12}L_{24}$. From the trajectory analysis, we found that ligand cluster size of 24 which corresponds to the experimentally observed $M_{12}L_{24}$ [7,8] is the most stable cluster size. The average coordination number is close to 4 at the experimental temperature. The average coordination number of 4 also corresponds to the feature of experimentally observed $M_{12}L_{24}$ [7,8]. In the metal-ligand clusters with ligand cluster size of 24 and average coordination number 4, two polyhedral frameworks with T_d and C_{3v} symmetry were mainly observed. The stereoisomer determined by X-ray crystallographic analysis has T_d symmetry [7,8,12,17,32–34]. These results support the utility of REMD method to predict self-assembled molecular structures. The framework with C_{3v} symmetry has a slightly higher probability than that with T_d symmetry. The potential energy of the framework with T_d symmetry is, however, more favorable

than that of the framework with C_{3v} symmetry. To discuss the thermodynamic stability of the stereoisomers more quantitatively, we need to use more accurate potential energy function including quantum effects of the metal-ligand coordination interactions. The work in this direction is under way.

Appendix A. Supplementary material

Supplementary data associated with this article can be found, in the online version, at https://doi.org/10.1016/j.cplett.2018.10.059.

References

[1] M. Fujita, Metal-directed self-assembly of two- and three-dimensional synthetic receptors, Chem. Soc. Rev. 27 (1998) 417–425.
[2] D.A. McMorran, P.J. Steel, The first coordinatively saturated, quadruply stranded helicate and its encapsulation of a hexafluorophosphate anion, Angew. Chem. Int. Ed. Engl. 37 (1998) 3295–3297.
[3] P. Liao, B.W. Langloss, E.R.K.A.M. Johnson, F.S. Tham, R.R. Julian, R.J. Hooley, Two-component control of guest binding in a self-assembled cage molecule, Chem. Commun. 46 (2010) 4932–4934.
[4] K. Suzuki, M. Tominaga, M. Kawano, M. Fujita, Self-assembly of an M_6L_{12} co-ordination cube, Chem. Commun. 13 (2009) 1638–1640.
[5] B. Moulton, J. Lu, A. Mondal, M.J. Zaworotko, Nanoballs: nanoscale faceted polyhedra with large windows and cavities, Chem. Commun. 9 (2001) 863–864.
[6] M. Eddaoudi, J. Kim, J. Wachter, H. Chae, M. O'keeffe, O. Yaghi, Porous metal-organic polyhedra: 25 Å cuboctahedron constructed from 12 $Cu_2(CO_2)_4$ paddle-wheel building blocks, J. Am. Chem. Soc. 123 (2001) 4368–4369.
[7] M. Tominaga, K. Suzuki, M. Kawano, T. Kusukawa, T. Ozeki, S. Sakamoto, K. Yamaguchi, M. Fujita, Finite, spherical coordination networks that self-organize from 36 small components, Angew. Chem. Int. Ed. 43 (2004) 5621–5625.
[8] Q.-F. Sun, J. Iwasa, D. Ogawa, Y. Ishido, S. Sato, T. Ozeki, Y. Sei, K. Yamaguchi, M. Fujita, Self-assembled $M_{24}L_{48}$ polyhedra and their sharp structural switch upon subtle ligand variation, Science 328 (2010) 1144.
[9] D. Fujita, Y. Ueda, S. Sato, H. Yokoyama, N. Mizuno, T. Kumasaka, M. Fujita, Self-assembly of $M_{30}L_{60}$ icosidodecahedron, Chem 1 (2016) 91–101.
[10] D. Fujita, Y. Ueda, S. Sato, N. Mizuno, T. Kumasaka, M. Fujita, Self-assembly of tetravalent Goldberg polyhedra from 144 small components, Nature 540 (2016) 563–566.
[11] S. Sato, J. Iida, K. Suzuki, M. Kawano, T. Ozeki, M. Fujita, Fluorous nanodroplets structurally confined in an organopalladium sphere, Science 313 (2006) 1273.
[12] D. Fujita, K. Suzuki, S. Sato, M. Yagi-Utsumi, Y. Yamaguchi, N. Mizuno, T. Kumasaka, M. Takata, M. Noda, S. Uchiyama, K. Kato, M. Fujita, Protein en-capsulation within synthetic molecular hosts, Nat. Commun. 3 (2012) 1093.
[13] K. Suzuki, S. Sato, M. Fujita, Template synthesis of precisely monodisperse silica nanoparticles within self-assembled organometallic spheres, Nat. Chem. 2 (2010) 25–29.
[14] S. Sato, Y. Yoshimasa, D. Fujita, M. Yagi-Utsumi, T. Yamaguchi, K. Kato, M. Fujita, A self-assembled spherical complex displaying a gangliosidic glycan cluster capable of interacting with amyloidogenic proteins, Angew. Chem. Int. Ed. 54 (2015) 8435–8439.
[15] M. Yoneya, T. Yamaguchi, S. Sato, M. Fujita, Simulation of metal-ligand self-assembly into spherical complex M_6L_8, J. Am. Chem. Soc. 134 (2012) 14401–14407.
[16] M. Yoneya, S. Tsuzuki, T. Yamaguchi, S. Sato, M. Fujita, Coordination-directed self-assembly of $M_{12}L_{24}$ nanocage: effects of kinetic trapping on the assembly process, ACS Nano 2 (2014) 1290–1296.
[17] D. Fujita, H. Yokoyama, Y. Ueda, S. Sato, M. Fujita, Geometrically restricted intermediates in the self-assembly of an $M_{12}L_{24}$ cuboctahedral complex, Angew. Chem. Int. Ed. 54 (2015) 155–158.
[18] Y. Sugita, Y. Okamoto, Replica-exchange molecular dynamics method for protein folding, Chem. Phys. Lett. 314 (1999) 141–151.
[19] S.G. Itoh, Y. Okamoto, Amyloid-β(29-42) dimer formations studied by a multi-canonical-multioverlap molecular dynamics simulation, J. Phys. Chem. B 112 (2008) 2767–2770.
[20] R. Urano, Y. Okamoto, Observation of helix associations for insertion of a retinal molecule and distortions of helix structures in bacteriorhodopsin, J. Chem. Phys. 143 (2015) 235101.
[21] H.H. Arefi, T. Yamamoto, Self-assembly of a model supramolecular polymer studied by replica exchange with solute tempering, J. Chem. Phys. 147 (2017) 211102..
[22] H. Kokubo, Y. Okamoto, Prediction of transmembrane helix configurations by

replica-exchange simulations, Chem. Phys. Lett. 383 (2004) 397–402.

[23] Y. Pang, Novel zinc protein molecular dynamics simulations: steps toward anti-angiogenesis for cancer treatment, J. Mol. Model. 5 (1999) 196–202.

[24] S. Yun-yu, W. Lu, W.V. Gunsteren, On the approximation of solvent effects on the conformation and dynamics of cyclosporin a by stochastic dynamics simulation techniques, Mol. Simul. 1 (1988) 369–383.

[25] I. Tironi, R. Sperb, P. Smith, W. van Gunsteren, A generalized reaction field method for molecular dynamics simulations, J. Chem. Phys. 102 (1995) 5451.

[26] J. Weeks, D. Chandler, H. Andersen, Role of repulsive forces in determining the equilibrium structure of simple liquids, J. Chem. Phys. 54 (1971) 5237.

[27] S. Pronk, S. Pall, R. Schulz, P. Larsson, P. Bjelkmar, R. Apostolov, M.R. Shirts, J.C. Smith, P.M. Kasson, D. van der Spoel, E.L.B. Hess, GROMACS 4.5: a high-throughput and highly parallel open source molecular simulation toolkit, Bioinformatics 29 (2013) 845–854.

[28] K.A. Feenstra, H.J.B.B. Hess, Improving efficiency of large time-scale molecular dynamics simulations of hydrogen-rich systems, J. Comput. Chem. 20 (1999) 786–798.

[29] E. Lindahl, B. Hess, D. van der Spoel, GROMACS 3.0: a package for molecular simulation and trajectory analysis, J. Mol. Model. 7 (2001) 306.

[30] R.G. Miller, The jackknife–a review, Biometrika 61 (1974) 1–15.

[31] Q.-F. Sun, S. Sato, M. Fujita, An $M_{12}(L^1)_{12}(L^2)_{12}$ cantellated tetrahedron: a case study on mixed- ligand self-assembly, Angew. Chem. Int. Ed. 53 (2014) 13510–13513.

[32] H. Yokoyama, Y. Ueda, D. Fujita, S. Sato, M. Fujita, Finely resolved threshold for the sharp $M_{12}L_{24}/M_{24}L_{48}$ structural switch in multi-component M_nL_{2n} polyhedral assemblies: X-ray, MS, NMR, and ultracentrifugation analyses, Chem. Asian J. 10 (2015) 2292–2295.

[33] C.J. Bruns, D. Fujita, M. Hoshino, S. Sato, J.F. Stoddart, M. Fujita, Emergent ion-gated binding of cationic host-guest complexes within cationic $M_{12}L_{24}$ molecular flasks, J. Am. Chem. Soc. 136 (2014) 12027–12034.

[34] K. Harris, Q.-F. Sun, S. Sato, M. Fujita, $M_{12}L_{24}$ spheres with endo and exo coordination sites: scaffolds for non-covalent functionalization, J. Am. Chem. Soc. 135 (2013) 12497–12499.